LA-UR- 11-04478

*Approved for public release; distribution is unlimited.*

*Title:* Simultaneous Photonic Doppler Velocimetry and Ultra-high Speed Imaging Techniques to Characterize The Pressure Output of Detonators

*Author(s):* Michael J. Murphy
Steven A. Clarke

*Intended for:* The Proceedings of the 17th Topical Conference on Shock Compression of Condensed Matter

Los Alamos
NATIONAL LABORATORY
EST. 1943

# SIMULTANEOUS PHOTONIC DOPPLER VELOCIMETRY AND ULTRA-HIGH SPEED IMAGING TECHNIQUES TO CHARACTERIZE THE PRESSURE OUTPUT OF DETONATORS

**Michael J. Murphy* and Steven A. Clarke***

** W-6 Detonator Technology, MS-P950, Los Alamos National Laboratory, Los Alamos, NM 87545*

**Abstract.** Detonator output directed into both ambient air and polymethylmethacrylate (PMMA) windows is simultaneously investigated using ultra-high speed, time-resolved imaging and photonic Doppler velocimetry (PDV) measurements. In air, one-dimensional measurements of detonator cup position are made from time-resolved image sequences and compared to time-integrated velocity curves obtained from the PDV data. The results demonstrate good agreement that validates using the two methods concurrently to measure the motion of the detonator free-surface. In PMMA windows, instantaneous shock velocities are calculated from 1-D time-resolved measurements of shock position and known velocity-Hugoniot data are utilized to map the shock velocity calculations to corresponding values of mass velocity and shock pressure. Simultaneous PDV data describing the motion of the detonator cup/PMMA interface are used to determine the mass velocity and pressure at the interface, and to compare to the mass and shock pressures calculated from the imaging data. Experimental results are in good agreement with empirical detonation- and shock-interaction calculations, as well as 1-D numerical simulations.
**Keywords:** Detonator, Shock Wave, PMMA, Ultra-High Speed, PDV
**PACS:** 62.50.Ef

## INTRODUCTION

In a typical detonator, a low-density initial pressing of explosive is directed into a higher density output pellet to enhance the overall output pressure of the detonator. The steady pressure state of reaction products behind the lead shock in a detonating explosive is referred to as the Chapman-Jouguet (C-J) state that is unique to the employed explosive at a given density. While it appears convenient to define detonator output by the C-J state of the output explosive, nearly all detonators contain some form of metal cup or lid that houses the explosive and interacts with the detonation wave to create a pressure state in the metal that differs from the C-J state. Since different metals shock up to different pressures when placed in contact with the same detonating explosive, appropriate characterization of detonator output quantified in terms of pressure must account for the detonation interaction with the inert cup material and not be based solely on detonation physics. In this work, detonator output is defined as the pressure state in the explosive cup material that interacts with the next component in the explosive assembly.

In order to establish a baseline performance of detonators, a diagnostic technique is developed that simultaneously employs specialized ultra-high speed imaging with surface velocimetry. The main interest in this work involves establishing a performance baseline for designing performance-matched detonators based on experimentally-observed equivalencies. In the ensuing discussion, experimental results describing the shocked state of a nickel cup on a prototype detonator are compared to 1-D numerical simulations, as well as 1-D detonation- and shock-interaction calculations made from empirical equations of state.

## EXPERIMENTAL

A prototype detonator employing a 1.6 g/cm$^3$ output pellet of PBX 9407 pressed into a 241 $\mu$m thick nickel cup (N02200) is investigated. Detonator output is directed into both ambient air and polymethylmethacrylate (PMMA) samples that behave as dynamic witness plates for the imaging experiments and window materials for the photonic Doppler velocimetry (PDV) experiments. The PMMA samples are machined from the same stock material to avoid variations in their physical properties, and the density and longitudinal sound velocity of the samples are consistently measured as 1.187 $\pm$ 0.001 g/cm$^3$ and 2.73 $\pm$ 0.03 mm/$\mu$s.

The ultra-high speed imaging system is fundamentally an inline schlieren photography setup without an implemented cutoff and is a variation of the system described in [1]. Notable upgrades include a SIMD ultra-high speed framing camera (Specialised Imaging) for improved image quality, a 5 Watt continuous-wave laser backlight with spoiled coherence (Spectra-Physics Reveal 5) for more uniform illumination, and a more robust imaging configuration for precise shot reproducibility. Detonator output is visualized without the use of a schlieren cutoff due to large deflection angles that result from interaction of the collimated backlight with detonator-driven shock waves.

A standard PDV system is employed that utilizes a single 1550 nm laser (IPG Photonics) for target illumination and a collimating probe that produces a 600 $\mu$m nominal spot size on the target. In each experiment the nickel cup behaves as the moving reflector, and the data is reduced using fast Fourier transform (FFT) analysis.

## RESULTS AND DISCUSSION

Imaging results are included in figure 1, where top and bottom sequences depict detonator output into air and PMMA, respectively recorded using 50 ns and 75 ns inter-framing. Only the first eight frames of the recorded sixteen-frame image sequences are displayed for compactness.

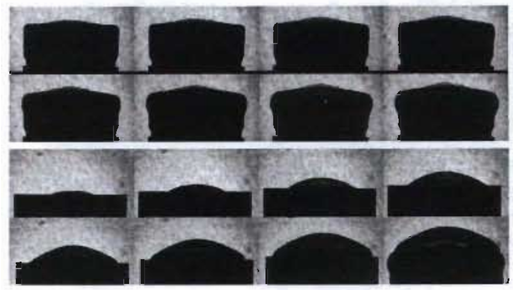

**FIGURE 1.** Image sequences of detonator output into (top) air using 50 ns inter-framing and (bottom) PMMA using 75 ns inter-framing.

From the air sequence, one-dimensional measurements of nickel free-surface position along the detonator centerline are paired with corresponding exposure times, and a power-law fit of the form $y_{fs}(t) = a(t-b)^c$ is applied to the measurements. The simultaneous PDV data is reduced to a spectrogram and displayed in figure 2, where the thick dashed line corresponds to $\mathrm{d}y_{fs}(t)/\mathrm{d}t$. Both the imaging and PDV data are in general quantitative agreement, and suggest the free-surface of the nickel cup is accelerating as an explosively-driven flyer. To better assess the agreement, a velocity time-history is extracted from the PDV spectrogram by Gaussian fitting the data in each FFT window and specifying the fit centroid as the value of the measurement (black dots in figure 2). The resulting velocity curve is integrated in time and plotted with the imaging data in figure 3, and the close agreement validates using the two methods concurrently to measure the motion of the detonator free-surface.

The shock state of the nickel cup is determined from the PDV data by extracting the initial jump in the measured free-surface velocity ($v_{fs}$) and noting that $v_{fs}$ is the sum of mass velocities due to shock compression ($u_p$) and material rarefaction ($u_r$). From [2], $u_p = u_r$ to within less than 3% for many metals compressed up to 50 GPa; hence, $u_p = v_{fs}/2$ is taken with confidence. Empirical Hugoniot data for nickel having average density 8.875 g/cm$^3$ is provided in [3] that suggests a linear $U_s - u_p$ Hugoniot with parameters $C_0 = 4.60$ mm/$\mu$s and $s = 1.44$. By invoking momentum conservation, $u_p$ is mapped to shock pressure as $p_s(u_p) = \rho_0 (C_0 + s u_p) u_p$, and results from two experiments are summarized in table 1, where the pressure in the nickel cup is determined as 42.6 and 42.1 GPa.

Turning to the PMMA experiments, the image sequence in figure 1 visualizes a detonator driven shock

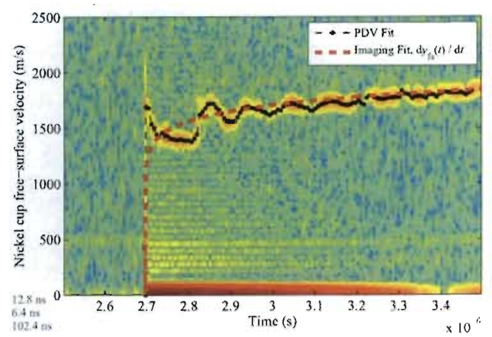


**FIGURE 2.** PDV spectrogram describing the explosively-driven motion of the nickel cup free-surface accelerating into laboratory air.

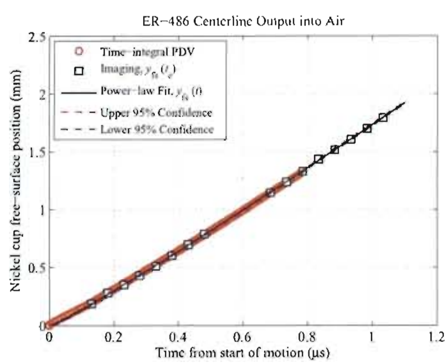


**FIGURE 3.** Centerline imaging and PDV measurements.

wave propagating into uncompressed PMMA. Vertical shock position measurements are made along the detonator centerline, and the same power-law equation is fit to the data. In this case, the resulting equation describes the temporal evolution of shock position from which instantaneous shock velocity ($U_s$) can be obtained by taking the time-derivative of the fit equation. Identical to the nickel analysis, empirical Hugoniot data for PMMA having average density 1.186 g/cm$^3$ and longitudinal sound speed 2.72 mm/$\mu$s is provided in [3] that yields a linear $U_s - u_p$ Hugoniot with parameters $C_0 = 2.603$ mm/$\mu$s and $s = 1.518$, for $u_p < 2.55$ mm/$\mu$s. Hence, the equation for shock velocity obtained from the imaging data is mapped to particle velocity using the $U_s - u_p$ Hugoniot, and further mapped to shock pressure through

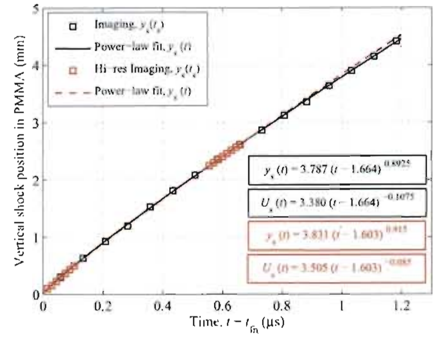


**FIGURE 4.** Centerline shock position in PMMA.

momentum conservation.

Vertical shock position measurements for two experiments are plotted in figure 4, where very good agreement between the measurements is observed that supports the reproducibility of both the detonator output and the measuring system. Corresponding power-law fits are included in figure 4, and the resulting mappings to shock pressure are plotted in figure 5. An apparent limitation of fitting data describing decelerating motion with a power-law model is that the derivative of the fit equation asymptotes to infinity at zero time, which a) does not allow the finite-strength of the shock at the nickel/PMMA interface to be determined and b) provides reason to question the fidelity of the pressure mapping at times very close to zero. As a result, the simultaneous PDV records describing the motion of the nickel/PMMA interface are used to measure the intial shock state of the PMMA sample, while the imaging data describes the evolution of shock strength decay in the sample.

Figure 6 displays the reduced spectrogram from the PDV data recorded by viewing the nickel/PMMA interface through the sample as it shock compresses. There is scarce literature available that quantifies a PMMA window correction factor for 1550 nm PDV experiments, but numerous works have demonstrated that at visible wavelengths the correction is negligible up to window stresses of 22 GPa, as summarized in [4]. Accordingly, velocity histories obtained from the PDV data are considered measurements of the true interface velocity, and the initial velocity jump ($u_{\text{int}}$) corresponding to the C-J state of PBX 9407 interacting with the nickel cup is then extracted from the individual velocity histories as the transition

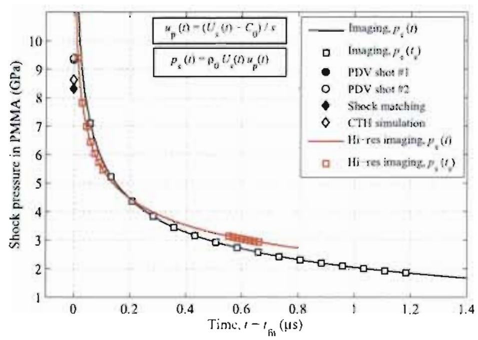


**FIGURE 5.** Centerline shock pressure in PMMA.

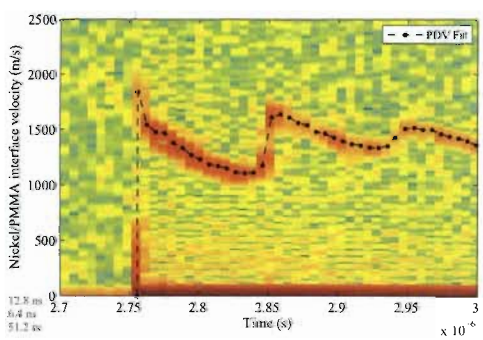


**FIGURE 6.** PDV spectrogram describing the explosively-driven motion of the nickel cup/PMMA window interface.

point between the initial rapid decay and the slower decay trend, following [5].

Initial jump velocities and corresponding pressure values for two PMMA experiments are summarized in table 1 as 9.35 and 9.40 GPa, and a comparison of the PDV measurements is made to 1-D numerical simulations performed using an Eulerian hydrocode (CTH [6]), and 1-D detonation- and shock-interaction calculations. Very good agreement is observed between all three methods, and we note the Hugoniot used for PBX 9407 reaction products is taken from [7], with C-J state parameters from [8]. We are actively seeking a more appropriate fit model to apply to the 1-D shock position measurements.

**TABLE 1.** Summary of results from PDV experiments, CTH simulations, and empirical calculations for detonator output into air and PMMA.

| *Variable* | *Experiment* | *CTH* | *Calculated* |
|---|---|---|---|
| | **Air** | | |
| $v_{fs}$ (mm/$\mu$s) | 1.660<br>1.643 | — | — |
| $u_p$ (mm/$\mu$s) | 0.830<br>0.822 | — | 0.825 |
| $p_s$ (GPa) | 42.6<br>42.1 | 42.9 | 42.4 |
| | **PMMA** | | |
| $u_{int}$ (mm/$\mu$s) | 1.577<br>1.583 | — | 1.458 |
| $p_{int}$ (GPa) | 9.35<br>9.40 | 8.64 | 8.33 |

## ACKNOWLEDGMENTS


Funding was provided by the Joint DOD/DOE Munitions Program. The authors wish to thank Michael Martinez for his technical assistance in implementing the PDV experiments, as well as Thomas Mason and Daniel Seegmiller for running the CTH simulations.


## REFERENCES


1. Clarke, S. A., Murphy, M. J., Landon, C. D., Mason, T. A., Adrian, R. J., Akinci, A. A., Martinez, M. E., and Thomas, K. A., *Proc. SPIE*, **6662** (2007).
2. Zhernokletov, M. V., and Glushak, B. L., *Material Properties under Intensive Dynamic Loading*, Springer, New York, 2006.
3. Marsh, S. P., *LASL Shock Hugoniot Data*, University of California Press, Berkeley, 1980.
4. Wise, J. L., and Chhabildas, L. C., Laser interferometer measurements of refractive index in shock-compressed materials, Tech. Rep. SAND-85-0310C, Sandia National Laboratories (1985).
5. Bouyer, V., Sheffield, S. A., Dattelbaum, D. M., Gustavsen, R. L., Stahl, D. B., Doucet, M., and Decaris, L., *AIP Conf. Proc.*, **1195**, 177–180 (2009).
6. McGlaun, J. M., Thompson, S. L., and Elrick, M. G., *International Journal of Impact Engineering*, **10**, 351–360 (1990).
7. Cooper, P. W., *Explosives Engineering*, Wiley-VCH, New York, 1996.
8. Dobratz, B. M., LLNL explosives handbook, Tech. Rep. UCRL-52997, Lawrence Livermore National Laboratory (1981).